

# Vaccinia Virus Morphogenesis Is Blocked by Temperature-Sensitive Mutations in the F10 Gene, Which Encodes Protein Kinase 2

SHUANGPING WANG AND STEWART SHUMAN\*

Program in Molecular Biology, Sloan-Kettering Institute, New York, New York 10021

Received 5 May 1995/Accepted 30 June 1995

**F**our previously isolated temperature-sensitive (*ts*) mutants of vaccinia virus WR (*ts28*, *ts54*, *ts61*, and *ts15*) composing a single complementation group have been mapped by marker rescue to the F10 open reading frame located within the genomic *Hind*III F DNA fragment. Sequencing of the F10 gene from wild-type and mutant viruses revealed single-amino-acid substitutions in the F10 polypeptide responsible for thermolabile growth. Although the *ts* mutants displayed normal patterns of viral protein synthesis, electron microscopy revealed a profound morphogenetic defect at the nonpermissive temperature (40°C). Virion assembly was arrested at an early stage, with scant formation of membrane crescents and no progression to normal spherical immature particles. The F10 gene encodes a 52-kDa serine/threonine protein kinase (S. Lin and S. S. Broyles, Proc. Natl. Acad. Sci. USA 91:7653–7657, 1994). We expressed a His-tagged version of the wild-type, *ts54*, and *ts61* F10 polypeptides in bacteria and purified these proteins by sequential nickel affinity and phosphocellulose chromatography steps. The wild-type F10 protein kinase activity was characterized in detail by using casein as a phosphate acceptor. Whereas the wild-type and *ts61* kinases displayed similar thermal inactivation profiles, the *ts54* kinase was thermosensitive in vitro. These findings suggest that protein phosphorylation plays an essential role at an early stage of virion assembly.

The DNA sequence of the vaccinia virus genome predicts that the virus encodes 199 polypeptides (13, 16). At least 70 vaccinia virus genes are dispensable for virus growth in cell culture (16). Genes essential for vaccinia virus replication have been defined by the isolation and characterization of conditionally lethal (temperature-sensitive [*ts*]) mutant viruses (4–7, 9, 11, 32). The combined mutant collection of R. Condit and M. Ensinger, consisting of 72 *ts* mutants of vaccinia virus strain WR, has been especially informative because nearly all of the 32 complementation groups have been assigned a crude physical map position based on marker rescue with wild-type DNA fragments (5, 6, 32). At least one isolate from each complementation group has been classified with respect to the patterns of macromolecular synthesis under nonpermissive growth conditions (6). Four broad phenotypes have been described: (i) DNA replication negative, (ii) abortive late protein synthesis, (iii) defective late protein synthesis, and (iv) normal. Normal mutants exhibit a wild-type pattern of DNA replication and protein synthesis at the nonpermissive temperature.

The normal phenotype is suggestive of mutation of a viral gene whose protein product might either participate in virion morphogenesis or be essential for establishment of the next round of infection (e.g., during virus penetration or the synthesis of early mRNAs by the virion-encapsidated RNA polymerase). Several normal mutants from the Condit collection have been mapped by marker rescue to individual viral genes. In some instances the gene product has been identified as an enzymatic component of the virus particle with a known or presumptive role in early transcription. Examples include the H4 protein, a subunit of the virion RNA polymerase (17, 36); the D6 protein, a subunit of the early transcription initiation factor (3, 20); and the I8 protein, an RNA helicase (12, 28). Other normal *ts* mutations map to constituent polypeptides of

the virion for which no enzymatic activity has yet been demonstrated. These include the D2, D3, and I7 proteins, mutations of which result in defective assembly of progeny virus particles at the nonpermissive temperature (10, 18).

There are currently 11 complementation groups of normal *ts* mutants from the Condit collection that have not been mapped to specific vaccinia virus genes. We anticipate that completion of the genetic assignments of these mutations will either illuminate the physiological roles of known viral proteins or define essential functions for some of the many virus-encoded proteins about which nothing is yet known beyond a predicted amino acid sequence. In this article, we present a molecular genetic and phenotypic analysis of four mutants (*ts28*, *ts54*, *ts61*, and *ts15*) isolated by Condit and assigned to a single complementation group (4, 5, 32). We demonstrate by electron microscopy that the *ts* growth phenotype is caused by a defect in virus assembly. The genetic lesions conferring the growth defect were mapped by marker rescue to the vaccinia virus F10 gene, encoding a virus-encapsidated protein kinase (21). One of the mutations (*ts54*) results in thermolability of protein kinase activity in vitro.

## MATERIALS AND METHODS

**Cells and viruses.** BSC40 cells were maintained in Dulbecco modified Eagle's medium (DME) supplemented with 5% fetal calf serum (FCS). Wild-type vaccinia virus WR was propagated in BSC40 cells grown at 37°C. Vaccinia virus mutants *ts12*, *ts15*, *ts28*, *ts54*, and *ts61* were kindly provided by R. Condit, University of Florida. *ts28* was subjected to two rounds of plaque purification in BSC40 cells grown at 31°C (permissive temperature) prior to amplification in monolayer cultures at 31°C. The other *ts* isolates were amplified in monolayers directly from virus suspensions obtained from the Condit laboratory. The thermolability of mutant virus stocks was verified by comparative titration on BSC40 cells at 31 and 40°C (nonpermissive temperature).

**Metabolic labeling.** Confluent BSC40 monolayers were infected with virus at multiplicity of infection of 10 at 40°C. The inoculum was removed after 30 min, and cells were washed once with medium and then overlaid with fresh DME–5% FCS. At various times postinfection, medium was removed, and cells were washed with methionine-free DME and then overlaid with methionine-free DME containing 30 or 120 µCi of [<sup>35</sup>S]methionine per ml (>800 Ci/mmol) for 30 min. In pulse-labeling experiments, this medium was removed and cells were

\* Corresponding author.

immediately lysed in situ by the addition of 0.15 ml of a solution containing 0.065 M Tris HCl (pH 6.8), 2% sodium dodecyl sulfate (SDS), 5%  $\beta$ -mercaptoethanol, and 10% glycerol. In pulse-chase experiments, the cells were washed twice with DME after the labeling medium was removed and then were overlaid with fresh medium containing unlabeled methionine. The monolayers were returned to incubate at 40°C and then lysed in situ after a 4- or 8-h chase. Lysates were stored at -20°C. Aliquots (30  $\mu$ l) were heated at 100°C for 5 min and then electrophoresed through a 10 or 12% polyacrylamide gel containing 0.1% SDS. Radiolabeled polypeptides were visualized by autoradiographic exposure of the dried gel.

**Plasmids and molecular cloning.** Plasmid pHind-F contains the 13.5-kbp *HindIII* F restriction fragment of vaccinia virus WR cloned into pUC13. Further subcloning was performed by insertion of gel-purified restriction fragments (see Fig. 1) into the polylinker of pBS(-) (Stratagene). Plasmids were named according to the restriction sites at the borders of the viral insert. DNAs used for marker rescue experiments were prepared by alkaline lysis and CsCl equilibrium centrifugation.

A plasmid containing the F10 open reading frame was generated as follows. Oligonucleotide primers complementary to the 5' and 3' flanks of the F10 open reading frame and containing restriction sites for *NdeI* and *BamHI*, respectively, were used to amplify the F10 gene from the pHind-F plasmid. The sequence of the 5' flanking primer was 5'-GCTTTTGTACACATATGGGTGGGCC; the 3' flanking primer was 5'-GACATTAGTAGGGATCCAATGTTGAGC. PCR was carried out with *Pfu* DNA polymerase. The PCR products were gel purified and cleaved with endonucleases *NdeI* and *BamHI*. The digestion products (a 510-bp *NdeI-NdeI* fragment from the 5' end of the F10 open reading frame and a 873-bp *NdeI-BamHI* fragment from the 3' end of F10) were gel purified. The 873-bp fragment, which included the coding region of F10 from amino acids 171 to 439) was inserted into plasmid pET16b (Novagen), which had been digested with *NdeI* and *BamHI*, to generate pet-F10(171-439). The 510-bp *NdeI* fragment of F10 was then inserted into pet-F10(171-439), which had been linearized with *NdeI*. The resulting plasmid, pet-F10, contained the entire F10 coding sequence. In this plasmid, a leader sequence encoding 10 tandem histidine codons is fused in frame to the 5' end of the F10 gene.

The genomic *HindIII* F fragment of mutant virus ts28 was gel purified from a *HindIII* digest of cytoplasmic DNA from BSC40 cells infected with ts28 at permissive temperature; this fragment was inserted into pBS(-), which had been cleaved with *HindIII*. A *BamHI-PstI* subclone derived from this ts28 pHind-F plasmid was used to determine the sequence of the ts28 F10 gene. Alternatively, the F10 genes from mutant viruses ts28, ts54, ts61, and ts15 were isolated by PCR amplification of total viral DNA (prepared from the cytoplasm of cells infected with ts virus at permissive temperature) using the flanking oligonucleotides used to prepare pet-F10. The amplified F10 fragments were digested with *NdeI* and *BamHI* and inserted into pET16b to generate the series pet-F10-ts. Several independent plasmid clones were isolated and sequenced for each mutant F10 allele. Sequencing of plasmid DNA was performed by the dideoxy nucleotide chain termination method. A T7 DNA polymerase-based sequencing kit (Sequenase, version 2.0) was used according to protocols supplied by the manufacturer (United States Biochemical).

**Marker rescue.** Confluent BSC40 cell monolayers (35-mm dishes) were infected with virus at a multiplicity of infection of 5 at 31°C. The inoculum was removed after 30 min, and cells were washed once with medium and overlaid with DME-5% FCS. After 30 min, cells were dislodged from the monolayer by treatment with 1 ml of 0.05% trypsin-0.53 mM EDTA. Suspended cells were mixed with 4 ml of DME and recovered by centrifugation for 5 min at 4°C in a clinical centrifuge. The pellet was washed with 0.5 ml of HBS (20 mM HEPES [N-2-hydroxyethylpiperazine-N'-2-ethanesulfonic acid] [pH 7.0], 150 mM NaCl, 0.7 mM Na<sub>2</sub>HPO<sub>4</sub>, 5 mM KCl, 6 mM dextrose) and centrifuged as before. The pellet was resuspended in 1 ml of cold HBS by pipetting and kept on ice. An aliquot (0.8 ml) of the suspension was transferred to a prechilled Bio-Rad 0.4-cm electrode gap cuvette. Plasmid DNA (10  $\mu$ g) was added to the cuvette (with mixing by pipetting), and the cuvette was chilled on ice for 10 min. The cuvette was pulsed at 200 V (capacitance, 960  $\mu$ F) in a Bio-Rad Gene Pulser equipped with a Bio-Rad Capacitance Extender and then kept on ice for 10 min. The suspension was diluted into 8 ml of medium at room temperature. An aliquot (3 ml) was then applied to a confluent cell monolayer of BSC40 cells (35-mm well) maintained at 40°C. After 2 days of incubation at 40°C, the cells were stained with 0.1% crystal violet in order to visualize plaques formed from infectious centers. Alternatively, in a two-step marker rescue assay, the monolayers were harvested by scraping and the yield of rescued virus was determined by titration on BSC40 monolayers at 40°C.

**Electron microscopy.** Confluent BSC40 cell monolayers (35-mm dishes) maintained at 40°C were infected with wild-type or ts virus at a multiplicity of infection of 10. The inoculum was removed after 30 min, and the cells were washed twice with medium and then overlaid with fresh DME-5% FCS. At 24 h postinfection, cells were dislodged by scraping and then spun in a clinical centrifuge. The supernatant was removed, and the cell pellet was placed immediately on ice. Cells were fixed initially in 2.5% glutaraldehyde and then in 2% osmium tetroxide. Specimens were dehydrated and then embedded in epoxy resin (Polybed 812). Thin sections were stained with uranyl acetate and lead citrate for visualization in a JEOL 1200 CX transmission electron microscope.

**Expression and purification of His-F10.** pET16-based expression plasmids for wild-type and ts F10 genes were transformed into *Escherichia coli* BL21(DE3).

Overnight cultures of *E. coli* BL21(DE3)/pet-F10 transformants were inoculated into 500 ml of Luria-Bertani medium containing 0.1 mg of ampicillin per ml and grown at 37°C until the *A*<sub>600</sub> reached approximately 0.6. Cultures were placed on ice for 30 min and adjusted to 2% ethanol and 0.2 mM IPTG (isopropyl- $\beta$ -D-thiogalactopyranoside). The cultures were then incubated at 18°C for 48 h with continuous shaking. Cells were harvested by centrifugation, and pellets were stored at -80°C. All subsequent procedures were performed at 4°C. Cell lysis was achieved by treatment of thawed, resuspended cells with lysozyme (0.2 mg/ml) and Triton X-100 (0.1%) in lysis buffer containing 50 mM Tris HCl (pH 7.5), 0.15 M NaCl, and 10% sucrose. Insoluble material was removed by centrifugation. The supernatants (approximately 50 ml) were mixed with 1 ml of Ni-nitrilotriacetic acid-agarose resin (Qiagen) for 2 h. The slurries were poured into a column and then washed with lysis buffer. The columns were eluted stepwise with IMAC buffer (20 mM Tris HCl [pH 7.9], 0.5 M NaCl, 1 mM phenylmethylsulfonyl fluoride, 10% glycerol) containing 5, 50, 100, or 200 mM imidazole. The polypeptide composition of the column fractions was monitored by SDS-polyacrylamide gel electrophoresis (SDS-PAGE). Fractions enriched for the expressed 54-kDa His-F10 polypeptides, which were eluted at 100 mM imidazole, were pooled and dialyzed against buffer A (50 mM Tris HCl [pH 8.0], 1 mM EDTA, 2 mM dithiothreitol (DTT), 0.1% Triton X-100, 10% glycerol). The dialysates were applied to 1-ml columns of phosphocellulose that had been equilibrated with buffer A. The columns were eluted stepwise with buffer A containing 0.1, 0.3, 0.5, or 1 M NaCl. The His-F10 protein was recovered in the 0.3 M NaCl fraction. Wild-type His-F10 was purified further by glycerol gradient sedimentation. An aliquot (0.2 ml) of the phosphocellulose fraction was applied to a 4.8-ml 15 to 30% glycerol gradient containing 0.5 M NaCl, 50 mM Tris HCl (pH 8.0), 1 mM EDTA, 2 mM DTT, and 0.1% Triton X-100. The gradients were centrifuged at 50,000 rpm for 20 h at 4°C in a Beckman SW50 rotor. Fractions were collected dropwise from the bottom of the tube. Protein concentrations were determined by using the Bio-Rad dye reagent with bovine serum albumin as a standard.

**Protein kinase assay.** Reaction mixtures (20  $\mu$ l) containing 50 mM Tris HCl (pH 7.5), 5 mM MgCl<sub>2</sub>, 1 mM DTT, 10  $\mu$ g of dephosphorylated  $\alpha$ -casein (Sigma), 50  $\mu$ M ATP, 10  $\mu$ Ci of [ $\gamma$ -<sup>32</sup>P]ATP (Amersham), and enzyme were incubated at 25°C for 10 min. The reaction was halted by addition of SDS; the samples were electrophoresed through a 10% polyacrylamide gel containing 0.1% SDS. Phosphorylated polypeptides were visualized by autoradiographic exposure of the dried gel. Phosphate transfer from [ $\gamma$ -<sup>32</sup>P]ATP to casein was quantitated either by scintillation counting of excised gel slices or by scanning the gel with a FUJIX BAS1000 Phosphorimager.

**Nucleotide sequence accession numbers.** The nucleotide sequence of F10 (WR) has been deposited in GenBank under accession number U32589. Other GenBank numbers are as follows: vaccinia virus strains Copenhagen and LIVP, M35027 and M57977, respectively; smallpox virus strains Bangladesh-1975 and India-1967, L22579 and X69198, respectively; swinepox virus, L22013.

## RESULTS

**Growth characteristics of mutant viruses.** Stocks of ts12, ts15, ts28, ts54, and ts61 prepared at the permissive temperature (31°C) were tested for their ability to form plaques at both 31°C and 40°C in BSC40 cells. The efficiency of plaque formation was reduced  $\geq$ 10,000-fold at the nonpermissive temperature. In contrast, the levels of plaque formation by wild-type virus at 31 and 40°C were equivalent.

**Marker rescue.** It was shown previously that ts28 could be restored to temperature-independent growth by marker rescue with a plasmid containing the entire *HindIII* F genomic fragment derived from wild-type virus (32). An annotated map of the 13.5-kbp F fragment, which includes 17 viral genes (16), is illustrated in Fig. 1. We mapped the ts28 mutation more precisely using an electroporation-based protocol for DNA-mediated marker rescue. Cells infected with ts28 were electroporated with plasmid DNA and plated onto uninfected cell monolayers maintained at the nonpermissive temperature. Successful marker rescue yields recombinant wild-type progeny from individual electroporated cells that were seeded onto the virgin monolayer; this was manifested as a plaque arising from each infectious center. No infectious centers were observed when monolayers were seeded with ts28-infected cells that had been electroporated without added DNA (Fig. 1). Marker rescue was achieved by electroporation with the pHind-F plasmid, containing the entire wild-type *HindIII* F fragment, but not with plasmid pHind-I, containing the 6.5-kbp wild-type *HindIII* I fragment (Fig. 2A). Rescue was also obtained with a *BamHI-HindIII* subclone corresponding to the

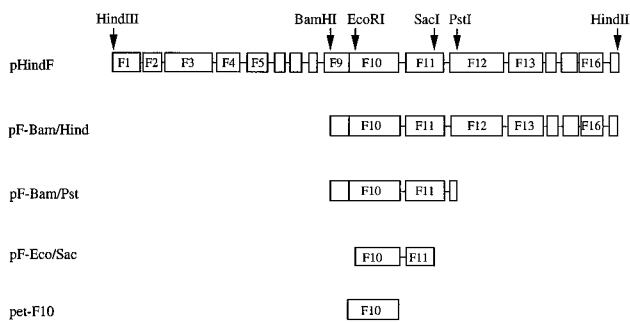


FIG. 1. Map of the genomic *Hind*III F fragment and subfragments used for marker rescue. Plasmid pHind-F contains the full 13.5-kbp *Hind*III F fragment cloned into pUC13. A physical and genetic map of the viral DNA insert is shown. *Hind*III restriction sites defining the borders of the viral DNA and internal sites for *Bam*HI, *Eco*RI, *Sac*I, and *Pst*I used in subcloning are indicated. Protein-encoding regions of the F fragment (boxed segments) are distinguished from noncoding regions (intervening line segments). Genes F1 through F16 are transcribed in the leftward direction, whereas F17 is transcribed rightward (13, 16). pF-Bam/Hind and pF-Bam/Pst contain subregions of the F fragment extending from the internal *Bam*HI site to either the terminal *Hind*III site or the internal *Sac*I site. pF-Eco/Sac includes portions of the F10 and F11 genes. pet-F10 contains the complete F10 open reading frame.

right half of the F fragment and including genes F9 to F17 (data not shown) and with a *Bam*HI-*Pst*I subclone that contained complete genes F10 and F11, along with portions of the F9 and F12 open reading frames (Fig. 1A). Marker rescue by an *Eco*RI-*Sac*I fragment further localized the *ts*28 mutation to a region including the amino portion of the F10 protein (residues 1 to 397) and the C terminus of the F11 gene product (Fig. 2B). Final assignment of the mutation was made by separately amplifying the F10 and F11 coding sequences by PCR and cloning the products into a pET-based vector. Plasmid pet-F10, containing the complete F10 gene but no coding sequence from the F11 gene, afforded marker rescue (Fig. 1B), whereas an F11-containing plasmid did not (data not shown). We concluded, therefore, that the genetic lesion of *ts*28 localized to the F10 gene. Similar analyses of *ts*54 and *ts*61 confirmed that these mutations also mapped to the F10 gene, i.e., rescue of growth was observed when *ts*54- or *ts*61-infected cells were electroporated with plasmid pHind-F, pF-Bam/Pst, pF-

*Eco*/Sac, or pet-F10 (Fig. 3). Parallel rescue of *ts*15 indicated that this mutation also mapped to F10 (not shown).

The extent of marker rescue of *ts*28, *ts*54, *ts*61, and *ts*15 viruses was quantitated by performing a two-step marker rescue procedure, in which the *ts* virus-infected cells were electroporated with pF-*Eco*/Sac DNA, plated on monolayers at 40°C, and then harvested at 48 h and titrated at the nonpermissive temperature. Transfection with pF-*Eco*/Sac DNA resulted in a virus yield of  $1 \times 10^6$  to  $2 \times 10^6$  PFU at 40°C, whereas *ts* virus-infected cells electroporated in parallel without plasmid DNA yielded less than  $10^3$  PFU (in the case of *ts*28, *ts*15, and *ts*54) or  $3 \times 10^3$  PFU (for *ts*61). The marker-rescued viruses were recovered and plated in parallel with wild-type virus at 40°C; plaque size and plaque morphology of the rescued viruses were indistinguishable from those of wild-type vaccinia virus.

We were unable to detect rescue of *ts*12, even when infected cells were electroporated with pHind-F, containing the entire genomic F fragment (not shown). We suspect that *ts*12 contains one or more separate *ts* mutations that map outside the genomic F fragment. (Note that the occurrence of a double *ts* mutation would not have impacted on the original assignment of this isolate to the same genetic complementation group as *ts*28, *ts*54, *ts*61, and *ts*15. Suspicions of a second *ts* lesion would not arise during complementation tests unless such lesions mapped to genes defined by other complementation groups in the collection.) We have therefore limited our subsequent studies to *ts*28, *ts*54, *ts*61, and *ts*15.

**Viral protein synthesis.** One-step growth experiments were performed with *ts*28, *ts*54, *ts*61, and *ts*15 at both 31°C and 40°C. Cells were harvested at 2, 12, 24, and 36 h after infection, and the production of infectious virus was assayed by titration at 31°C. The yield of *ts* progeny at 36 h at the permissive temperature was comparable to that of wild-type virus. No increase in the titer (over the 2-h background) was observed when infections with the *ts* viruses were performed at the nonpermissive temperature (not shown). Growth of wild-type virus did not vary significantly with temperature. The patterns of viral protein synthesis at nonpermissive temperature were analyzed by pulse-labeling synchronously infected cells with [ $^{35}$ S]methionine over a 12-h time course postinfection (Fig. 4). A normal temporal pattern of vaccinia virus gene expression was observed in cells infected with *ts*28, *ts*54, or *ts*61 at 40°C (Fig. 4). Hallmarks include the shutdown of host cell protein synthesis (e.g., the prominent 45-kDa cellular polypeptide denoted by the asterisk in Fig. 4) and the transition to late viral protein synthesis by 8 h postinfection. Late polypeptides are exemplified by the precursor forms of the major virion structural proteins (L in Fig. 4). Identical patterns of viral protein synthesis were observed in *ts*15-infected cells at 40°C (not shown). The polypeptide synthetic profiles for *ts*28, *ts*54, *ts*61, and *ts*15 were indistinguishable from that of wild-type virus at 40°C (not shown). Hence, all four members of the complementation group that could be rescued by the F10 gene displayed a normal phenotype with respect to viral protein synthesis.

**Defective processing of virion structural proteins at the nonpermissive temperature.** Three major structural proteins of the virion core—4a, 4b, and 25K—are encoded by the vaccinia virus A10, A3, and L4 genes, respectively. Each is synthesized at late times as a precursor polypeptide (p4a, p4b, or 28K) that is proteolytically processed to yield the mature species. Conversion of p4b to 4b and that of 28K to 25K both appear to entail single endoproteolytic events, whereas processing of p4a involves multiple internal cleavages that generate at least two polypeptides (4a and 23K) found in the core (31, 33, 35). The precursor polypeptides were readily identified

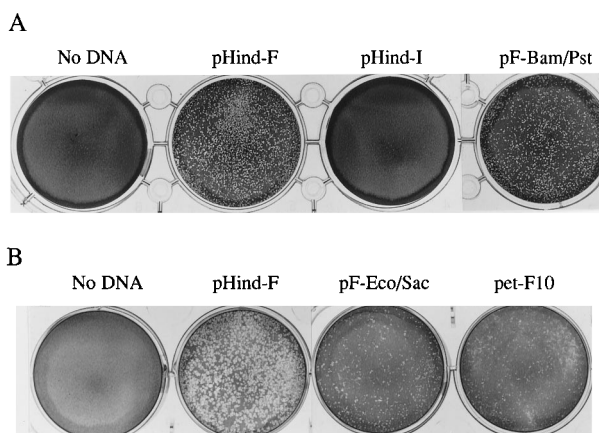


FIG. 2. Marker rescue of *ts*28. Electroporation-based marker rescue using supercoiled plasmid DNAs was performed as described in Materials and Methods. Photographs of the stained monolayers from two experiments (A and B) are shown. The no-DNA control entailed seeding the monolayers with virus-infected BSC40 cells that had been electroporated without added DNA.

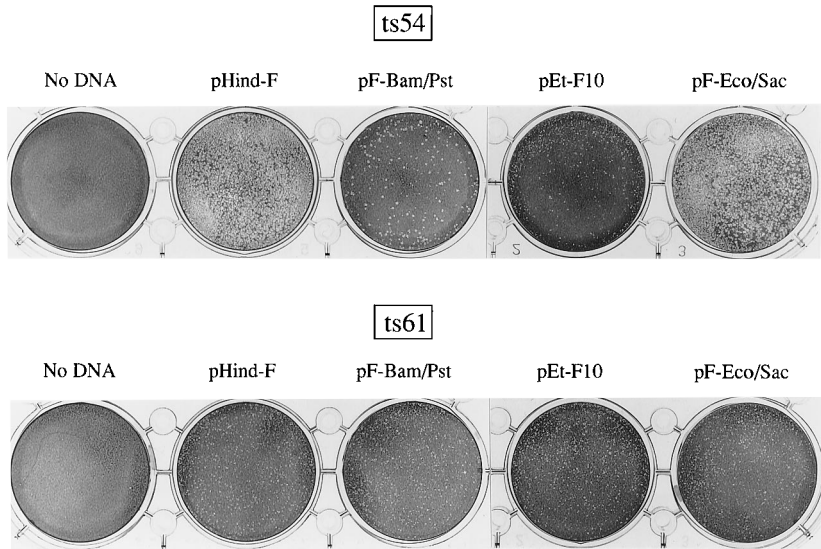


FIG. 3. Marker rescue of *ts*54 and *ts*61. Electroporation-based marker rescue was performed as described in Materials and Methods. Photographs of the stained monolayers are shown. The no-DNA control entailed seeding the monolayers with virus-infected BSC40 cells that had been electroporated without added DNA.

in [ $^{35}$ S]methionine pulse-labeling reactions performed during the late phase of vaccinia virus infection (e.g., 12 h postinfection [Fig. 4 and 5]) and were converted to mature forms during a chase of the wild-type virus-infected cells in the presence of unlabeled methionine (Fig. 5). Conversion was seen as a decrease in the labeled p4a and p4b polypeptides accompanied by the appearance of a doublet corresponding to 4a and 4b (asterisk in Fig. 5). (The 4a and 4b polypeptides were not resolved well in this gel, but other electrophoresis experiments confirmed that both species were present.) The precursors of 4a and 4b were synthesized in cells infected at 40°C with *ts*28, *ts*54, and *ts*15, but there was no apparent conversion to 4a and 4b, even after 8 h of chase (Fig. 5). In *ts*61-infected cells at

40°C, p4b was converted to 4b, but processing of p4a was inhibited (Fig. 5).

These results show that, although each of the *ts* mutants displayed some defect in precursor processing, the severity of the block to p4a and p4b processing varied among the F10 *ts* alleles. Disparate effects of vaccinia virus mutations on the processing of different precursor proteins have been noted previously (10, 38, 39). For example, *ts* mutations of vaccinia virus genes D2 and D3 have no effect of conversion of 28K to 25K, but they do block processing of p4a and delay the processing of p4b (10). A conditional null mutation of the viral D13 gene, which is required for virus assembly, also affects processing of p4a to a greater extent than p4b (39). A similar differential effect on p4a versus p4b was seen for a conditional null mutation in the gene encoding the 11-kDa virion core protein; this mutation also elicited a block to virion assembly (38). Because almost any mutation or drug treatment that blocks virus assembly also affects processing of the virion structural precursors, the latter finding provides a biochemical marker suggestive of a morphogenetic defect for the F10 *ts* mutant viruses at the nonpermissive temperature. This was evaluated directly by electron microscopy.

**Electron microscopy.** The mature vaccinia virion evolves in stages from microscopically well-characterized immature forms, which were apparent in electron micrographs of BSC40 cells infected with wild-type virus at 40°C (Fig. 6). The earliest of these are crescent-shaped spicule-coated viral membranes, which were observed either free in the cytoplasm (Fig. 6A) or associated with centers of electron-dense viroplasm (Fig. 6B). Spherical immature viral particles are formed upon closure of the membrane around the granular material (Fig. 6B). These spherical immature particles develop into mature brick-shaped virions, clusters of which were evident in wild-type-virus-infected cells (Fig. 6C). No mature progeny virions were observed in cells infected with *ts*28, *ts*54, or *ts*61 at the nonpermissive temperature. Cytoplasmic foci of viroplasm were visible, occasionally coalescing into sizable cytoplasmic inclusions, as shown in the low-power view of a cell infected with *ts*28 (Fig. 7A). Note that spherical immature particles were absent as well. Close scrutiny revealed only scant formation of

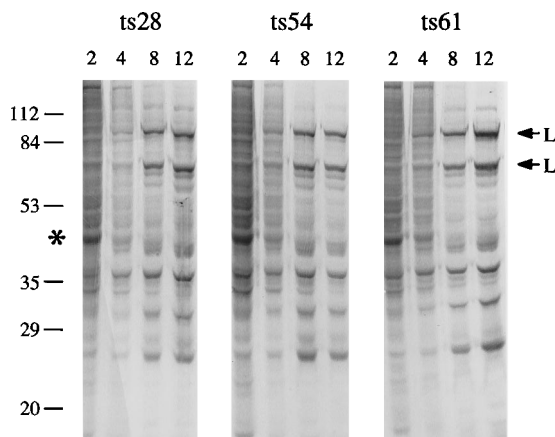


FIG. 4. Synthesis of viral proteins by *ts* mutant viruses. Virus-infected cells maintained at 40°C were pulse-labeled for 30 min with [ $^{35}$ S]methionine (30  $\mu$ Ci/ml of medium), and radiolabeled polypeptides were analyzed by SDS-PAGE as described in Materials and Methods. An autoradiograph of the gel is shown. The time at which the pulse-labeling was initiated (hours postinfection) is indicated above each lane. The positions and sizes (in kilodaltons) of coelectrophoresed protein standards are indicated on the left. A labeled polypeptide corresponding to the predominant 45-kDa host protein, actin (asterisk), and two abundant viral late proteins (L), corresponding to virion precursors p4a and p4b, are indicated.

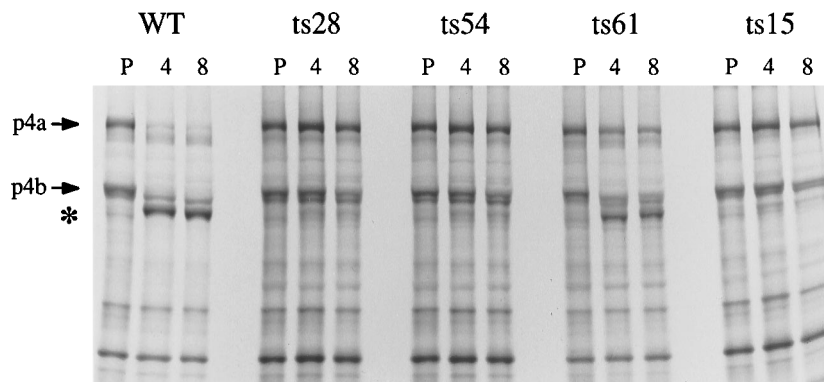


FIG. 5. Processing of virion structural proteins by *ts* mutant viruses. Virus-infected cells maintained at 40°C were pulse-labeled for 30 min with [<sup>35</sup>S]methionine (120  $\mu$ Ci/ml of medium) at 12 h postinfection and then either lysed in situ immediately after labeling (lanes P) or chased for the times indicated (in hours) in medium containing unlabeled methionine. Radiolabeled polypeptides were analyzed by SDS-PAGE. An autoradiograph of the gel is shown. The labeled polypeptides corresponding to the structural protein precursors p4a and p4b and their processed products 4a and 4b (an ill-resolved doublet in this gel) (asterisk) are indicated. WT, wild type.

viral membrane fragments in *ts*28-infected cells. Examples of such fragments are shown in Fig. 7B and C; these structures resemble the short crescents detected in wild-type-virus-infected cells. A similar situation applied to infection with *ts*54, in which we observed foci of viroplasm, occasionally accompanied by viral membrane fragments (Fig. 8A and B). Rarely, we observed spherical membranes, e.g., in *ts*61-infected cells in Fig. 8C; however, these spherical forms did not contain electron-dense viroplasm. There was no evidence of maturation beyond initial membrane formation. It should be emphasized that formation of viral membranes in *ts* virus-infected cells was far less extensive than in a wild-type vaccinia virus infection. Thus, the growth phenotypes of *ts*28, *ts*54, and *ts*61 could be attributed to a specific defect at an early stage of virus assembly.

**Sequence analysis of the wild-type and mutant F10 genes.** The wild-type F10 gene of the WR strain of vaccinia virus encodes a protein of 439 amino acids with a predicted molecular mass of 52 kDa (Fig. 9). The nucleotide sequence of F10

from vaccinia virus WR differed at 14 positions from the published sequence of the F10 gene of the Copenhagen strain (13). Twelve of the nucleotide changes were silent at the protein level. Two amino acid differences were noted between the WR and Copenhagen strains (Fig. 9). In order to fine map the *ts*28 mutation, the genomic *Hind*III F fragment of *ts*28 viral DNA was isolated from virus-infected cells and cloned into a pBS(−) plasmid vector; a *Bam*HI-*Pst*I subclone of this plasmid was employed for DNA sequencing. Dideoxy sequencing of the *ts*28 F10 gene revealed a single coding change (GTT to ATT) that resulted in a predicted Val-to-Ile substitution at residue 168 of the F10 polypeptide. The identical sequence was obtained when we analyzed two different plasmid clones obtained by PCR amplification of viral DNA from *ts*28-infected BSC40 cells. The molecular lesions of the *ts*54, *ts*61, and *ts*15 isolates were determined by sequencing individual plasmid clones obtained after PCR amplification from DNA isolated from *ts* virus-infected cells. Three different clones were sequenced for *ts*54, with each clone containing a single coding change (CCT

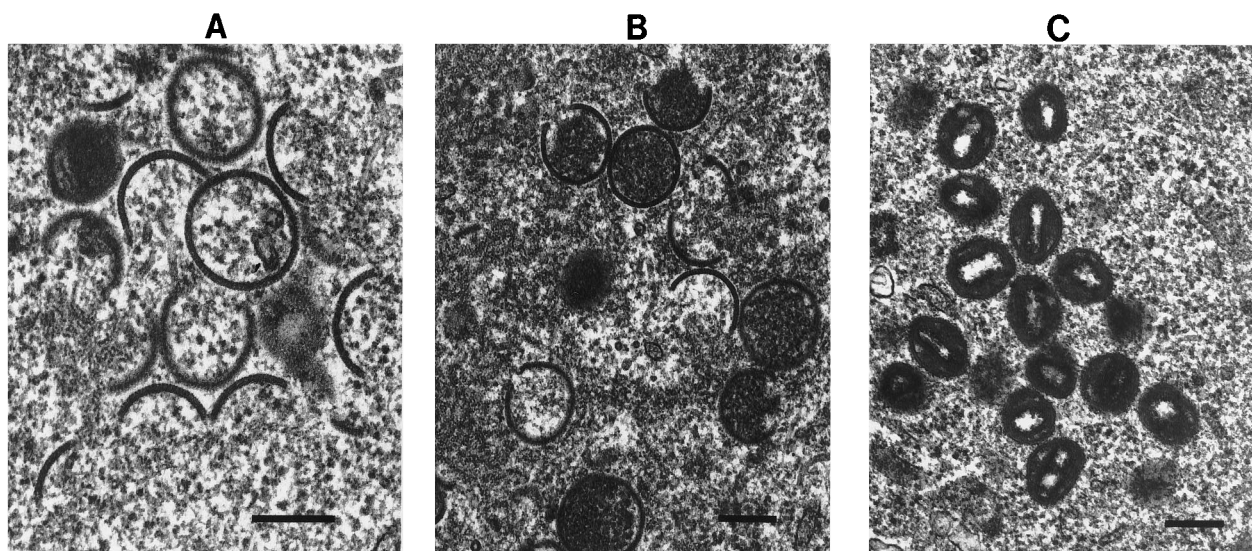


FIG. 6. Virus assembly assessed by electron microscopy. Cells infected with wild-type virus at 40°C were harvested at 24 h postinfection and analyzed by electron microscopy. Representative micrographs show several stages of viral morphogenesis. (A) Spicule-containing membrane crescents; (B) viral membranes and spherical immature virus particles containing electron-dense viroplasm; (C) a cluster of IMVs. Bars, 0.2  $\mu$ m.

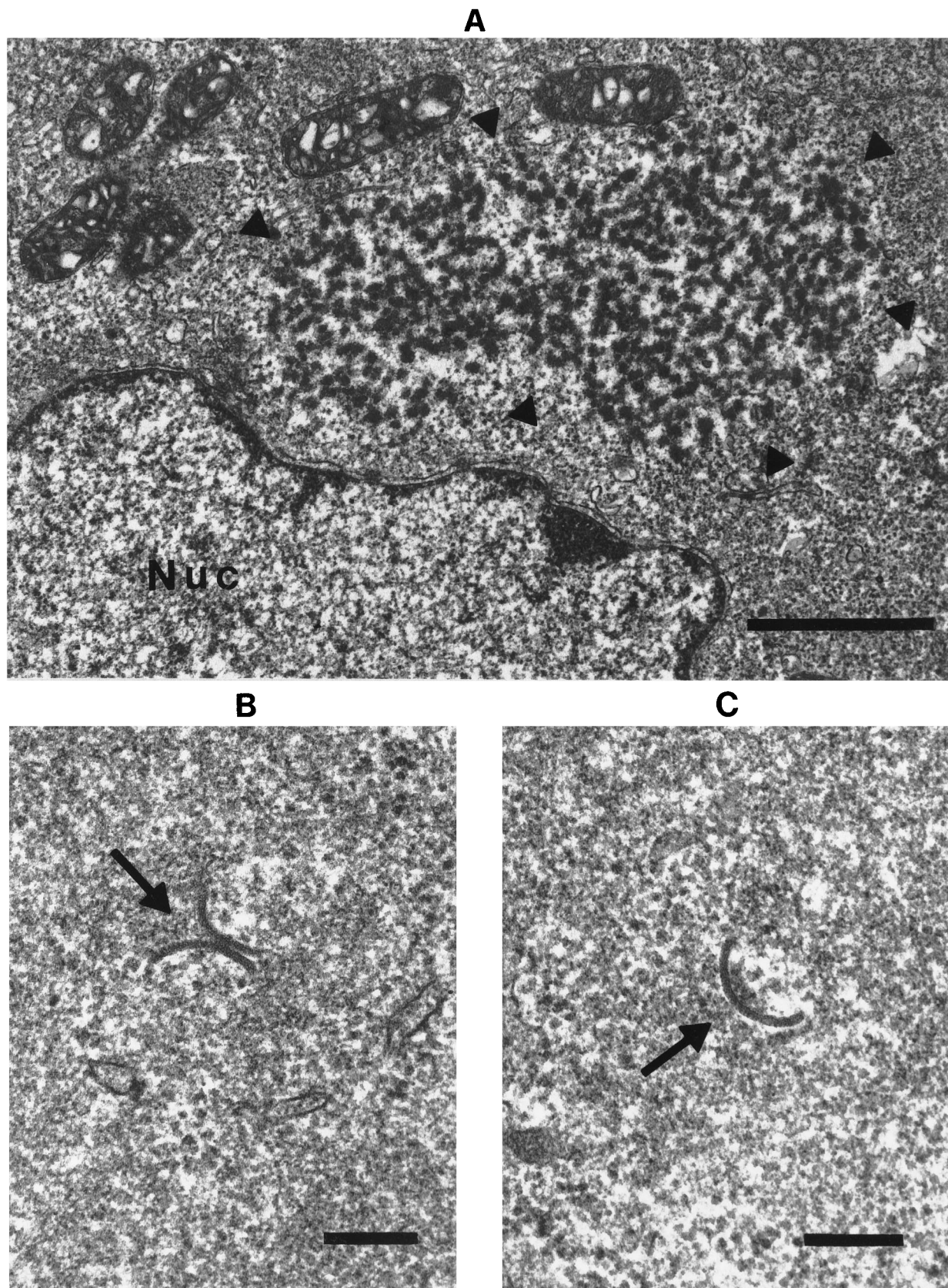


FIG. 7. Defective assembly of *ts*28. Cells infected with *ts*28 at 40°C were harvested at 24 h postinfection and analyzed by electron microscopy. (A) Cell nucleus (Nuc) and a large cytoplasmic focus of viroplasm (the borders of which are indicated by arrowheads). Several mitochondria, which are excluded from the viroplasm, can be seen at the upper left. Bar, 1  $\mu$ m. (B and C) Isolated fragments of crescent-shaped viral membranes (arrows) could be detected. Bars, 0.2  $\mu$ m.

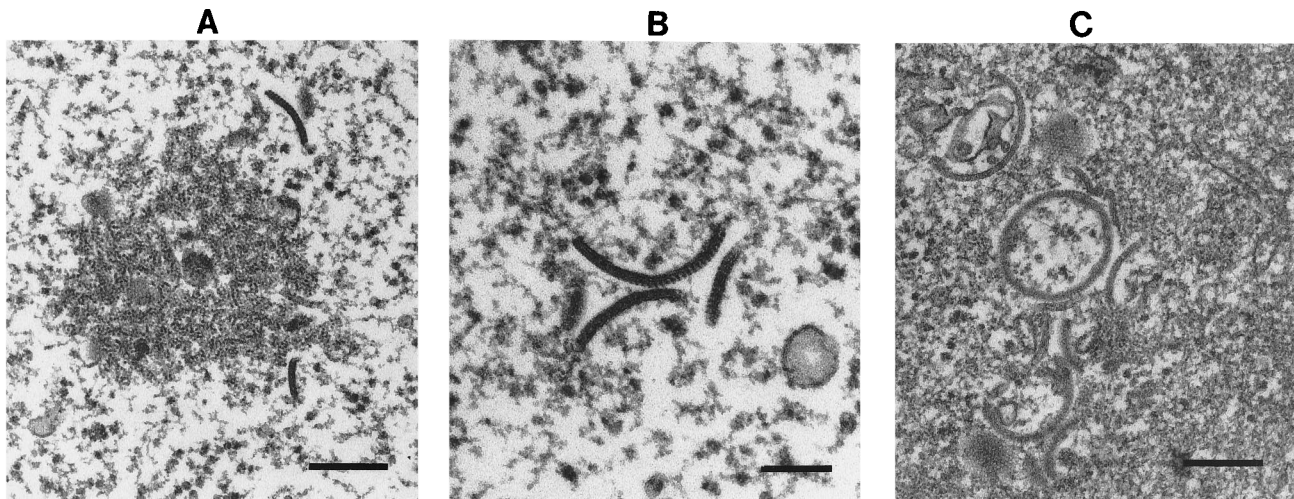


FIG. 8. Defective assembly of *ts54* and *ts61*. Cells infected with *ts54* (A and B) or *ts61* (C) at 40°C were harvested at 24 h postinfection and analyzed by electron microscopy. (A) A focus of electron-dense viroplasm flanked by two viral membrane fragments. Bar, 0.2  $\mu$ m. (B) A group of three viral membrane fragments. Bar, 0.1  $\mu$ m. (C) Membrane crescents and an apparently spherical membrane. These membranes do not enclose viroplasm (e.g., compare with Fig. 6B). Bar, 0.2  $\mu$ m.

to TCT) resulting in a Pro-to-Ser substitution at position 85. Three clones were sequenced for *ts61*, each containing a point mutation (GAA to AAA) resulting in a Glu-to-Lys substitution at position 123. Each of three clones derived from *ts15* contained a coding change (CCC to TCC) that produced a Pro→Ser substitution at residue 131. All F10 clones derived from *ts28*, *ts54*, *ts61*, and *ts15* (originating in the Condit laboratory) also contained a single silent base change relative to the wild-type WR sequence (which was obtained by sequencing a genomic clone of vaccinia virus WR originally constructed by M. Merchlinsky, National Institutes of Health); we attribute this silent change (AAC to AAT at the codon for Asn-33) to natural sequence variation among WR stocks grown in different laboratories.

A BLAST search of the NCBI database indicated that the F10 protein was most highly related to protein homologs encoded by other poxviruses, particularly the 439-amino-acid proteins of two strains of smallpox virus, variola Bangladesh and variola India (434 identical amino acids each) (Fig. 9). The LIVP strain of vaccinia virus encodes a 405-amino-acid F10 homolog that has a deletion of a 33-amino-acid internal segment (corresponding to residues 18 to 50 in the WR polypeptide) (Fig. 9). The swinepox virus homolog is identical at 314 positions to WR F10 and is punctuated by two single-residue insertions (Fig. 9). The F10 residues Pro-85, Pro-131, and Val-167, which when mutated confer temperature-sensitive growth are strictly conserved in each of the poxvirus proteins, whereas Glu-123, which is conserved among orthopoxviruses, is substituted by Asp in swinepox virus.

The database search also highlighted sequence similarities to a large number of protein kinases. (Three conserved kinase motifs in the F10 protein are underlined in Fig. 9.) Although it has been known for over 20 years that vaccinia virus particles contain a protein kinase activity (26) and the resemblance of F10 to kinases has been noted during genomic sequencing (13, 16), only recently has it become clear that the major kinase activity in the virion is encoded by the F10 gene. The virion kinase was identified by Lin and Broyles as the F10 gene product on the basis of the peptide sequence of the purified enzyme (21). The F10 protein was named vaccinia protein kinase 2, to distinguish it from the 300-amino-acid B1 gene product, which had been shown previously to be a serine/

threonine kinase (22, 27). The F10 and B1 kinases are not well conserved at the amino acid sequence level; their similarity is limited to the kinase motifs underlined in Fig. 9.

The DNA sequence of the F10 gene suggests that F10 is probably expressed at late times during vaccinia virus infection. For example, the ATG codon of the F10 protein is situated within a TAAATG sequence; the TAAAT motif is an essential component of a vaccinia virus late promoter, and the close proximity of TAAAT to the translation start site is a common feature of late genes (8). Furthermore, the F10 gene of vaccinia virus strain WR contains two internal TTTTNT motifs that specify termination of early gene transcription. Such motifs tend to be excluded from the coding sequence of viral early genes but are usually detected with late coding sequences because this signal is not recognized as a terminator during late transcription.

**Purification and characterization of recombinant F10 kinase.** In order to study the catalytic properties of vaccinia virus protein kinase 2 and to assess the biochemical consequences of the *ts* missense mutations, we expressed the F10 protein in bacteria. An inducible T7 RNA polymerase-based vector in which a short histidine-rich amino-terminal leader segment was fused to the F10 polypeptide was constructed. The expression plasmid was introduced into *E. coli* BL21(DE3), a strain that contains the T7 RNA polymerase gene under the control of a *lacUV5* promoter. Expression of the His-F10 polypeptide was induced by IPTG. Preliminary experiments indicated that solubility of the expressed His-F10 was improved by growing the bacteria at 18°C during IPTG induction (not shown). The His tag allowed for rapid enrichment of His-F10 due to the affinity of the tag for immobilized nickel. Soluble lysate was applied to Ni-agarose and step eluted with increasing concentrations of imidazole. SDS-PAGE analysis revealed a 54-kDa polypeptide eluted at 100 mM imidazole; this polypeptide was not recovered when lysates of induced BL21(DE3) carrying the pET16 vector were subjected to the same Ni-agarose chromatography procedure (not shown). The Ni-agarose His-F10 preparation catalyzed the transfer of  $^{32}$ P<sub>i</sub> from [ $\gamma$ - $^{32}$ P]ATP to casein, thereby confirming the observation of Lin and Broyles (with a glutathione S-transferase-F10 fusion protein) that recombinant F10 was catalytically active (see below) (21). His-F10 was purified further by adsorption to phosphocellulose and step elution with salt. Protein kinase activity was recovered

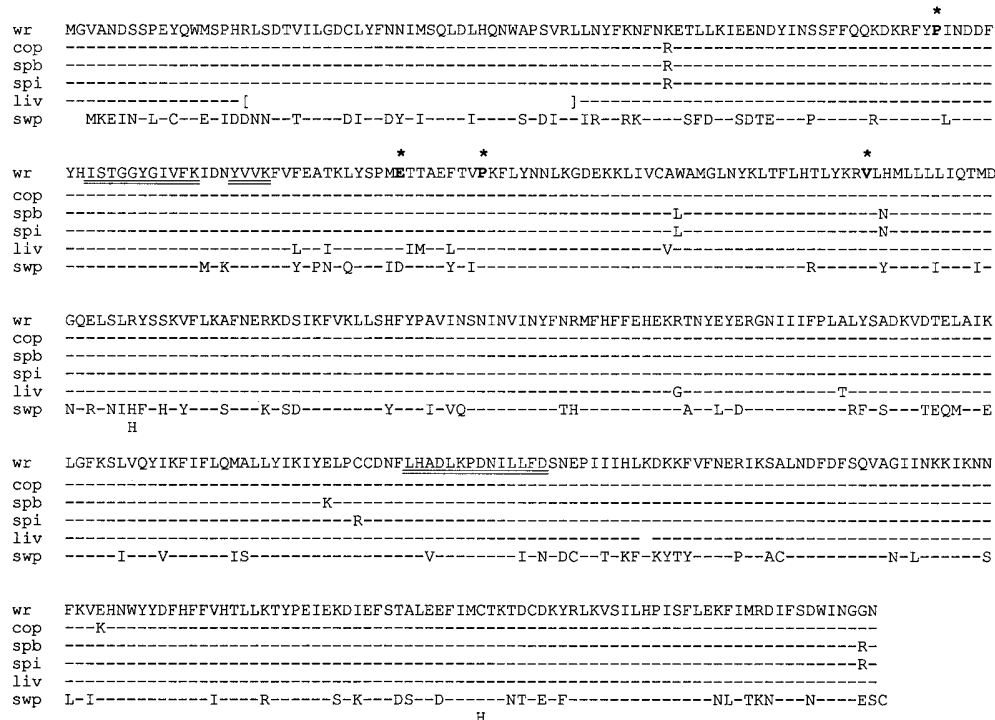


FIG. 9. Sequence of the F10 protein and locations of amino acid changes responsible for *ts* growth. The amino acid sequence of the 429-amino-acid F10 polypeptide encoded by wild-type vaccinia virus WR (wr) is shown aligned with the homologous polypeptides encoded by related poxviruses, including vaccinia virus strain Copenhagen (cop), smallpox virus (variola major) strain Bangladesh-1975 (spb), smallpox virus strain India-1967 (spi), vaccinia virus strain LIVP (liv), and swinepox virus (swp). Amino acids identical to those in the WR F10 protein are indicated by dashes. Divergent residues are indicated. A segment of the F10 protein that has apparently been deleted in the LIVP strain of vaccinia virus is demarcated by brackets. Two inserted residues in the swinepox homolog are indicated below the swinepox polypeptide sequence. Asterisks, amino acid residues in WR F10 that are mutated in vaccinia viruses *ts*54 (Pro-85), *ts*61 (Glu-123), *ts*15 (Pro-131), and *ts*28 (Val-168). Regions of the F10 protein that are conserved among numerous protein kinase family members are underlined.

in the 0.3 M NaCl fraction (see Fig. 11A), which was nearly homogeneous with respect to the 54-kDa His-F10 polypeptide (Fig. 10). The phosphocellulose preparation was centrifuged through a 15 to 30% glycerol gradient in 0.5 M NaCl. Protein kinase activity sedimented as a single peak (Fig. 11A) coincident with the sedimentation profile of the His-F10 polypeptide (Fig. 11B). A sedimentation coefficient of 4S (relative to catalase and cytochrome *c* centrifuged in parallel [not shown]) suggested that the vaccinia virus protein kinase was a monomer.

Further characterization of the F10 protein kinase was performed with the phosphocellulose enzyme fraction, with ATP as the phosphate donor and casein as the phosphate acceptor. The major phosphorylated reaction product was a 32-kDa polypeptide corresponding to casein (Fig. 11A). A minor phosphorylated species, migrating diffusely at about 70 kDa, was also detected. Formation of this labeled product, which was noted also by Lin and Broyles (21), depended on addition of casein and was presumed to represent a contaminating polypeptide in the casein preparation. Phosphoryl transfer from [ $\gamma$ -<sup>32</sup>P]ATP to casein was linear with time up to at least 20 min of incubation at 25°C (Fig. 12) and varied linearly with input enzyme (Fig. 13A). The kinase was active from pH 6.0 to 9.0 in Tris buffer (not shown). Kinase activity depended absolutely on a divalent cation and was optimal at 5 to 10 mM MgCl<sub>2</sub> (Fig. 14A). Manganese (5 mM) was equivalent to magnesium in supporting casein phosphorylation, whereas cobalt was less effective. Copper, calcium, and zinc supported much lower levels of activity (Fig. 14B). Kinase activity increased with ATP concentration from 10 to 50  $\mu$ M and leveled off thereafter (Fig. 12B); a  $K_m$  of 30  $\mu$ M ATP was calculated from

a double-reciprocal plot of the data. Activity was proportional to the amount of phosphate acceptor, with saturation achieved at 10  $\mu$ g of input casein (Fig. 12C). We calculated from the protein titration data (Fig. 13A) that His-F10 catalyzed a molar excess of protein phosphorylation relative to input protein (30 mol of phosphate incorporation into casein per mol of His-F10 during a 10-min reaction). This calculation was based on the protein concentration of the phosphocellulose preparation and the assumptions that (i) the His-F10 preparation was homogenous, (ii) the active form of the His-tagged enzyme was a 54-kDa monomer, and (iii) all enzyme molecules were catalytically active.

Incubation of purified His-F10 with [ $\gamma$ -<sup>32</sup>P]ATP and magnesium in the absence of casein resulted in label transfer to a single 54-kDa polypeptide; we attributed this to autophosphorylation. Note that native F10 kinase purified from vaccinia virions also catalyzed autophosphorylation (21). The extent of autophosphorylation by recombinant His-F10 was proportional to input protein (Fig. 13B). Higher levels of His-F10 were required to detect autophosphorylation than the levels required to detect phosphorylation of casein (compare Fig. 13A and B). We estimated that approximately 0.04 mol of autophosphorylation occurred per mol of His-F10.

**Kinase activity of *ts*61 and *ts*54 His-F10 proteins.** The F10 proteins encoded by the *ts*61 and *ts*54 alleles were expressed in bacteria as His-tagged fusions and purified by the same procedure as that used for wild-type His-F10. The extent of purification at the phosphocellulose step was comparable to that of the wild-type protein, as shown by SDS-PAGE (Fig. 11). *ts*61 His-F10 was nearly homogeneous with respect to the 54-kDa

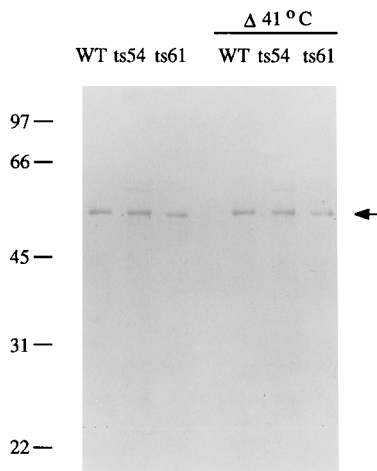


FIG. 10. Polypeptide composition of purified His-F10. Wild-type (WT), *ts54*, and *ts61* His-F10 proteins were expressed in bacteria and purified by Ni-agarose and phosphocellulose column chromatography steps. Aliquots (1.5 µg of protein) of the phosphocellulose fractions were denatured with SDS and analyzed by SDS-PAGE; also analyzed in parallel were samples of the protein fractions that had been incubated for 10 min at 41°C prior to SDS denaturation. Polypeptides were visualized by staining with Coomassie blue dye. The polypeptide corresponding to His-F10 is indicated (arrow). The positions and sizes (in kilodaltons) of coelectrophoresed marker proteins are indicated on the left.

polypeptide, whereas *ts54* His-F10 included a minor contaminant of 60 kDa (Fig. 10). (Initial attempts to express the *ts28* protein in bacteria were frustrated by low yield of soluble protein). The *ts61* and *ts54* proteins readily phosphorylated casein, and activity was proportional to input enzyme (Fig. 13A). The specific activity of the *ts61* His-F10 preparation was about half that of the wild-type F10 preparation (Fig. 13A). The specific activity of the *ts54* protein was about 30% of that of the wild type (Fig. 13A). Both mutant proteins were capable of autophosphorylation in the absence of casein; the specific activities in autophosphorylation were in the same range as that of wild-type His-F10 ( $\pm 40\%$ ) (Fig. 13B). (Because the extent of autophosphorylation by all F10 proteins was very low compared with casein phosphorylation, we are reluctant to attribute significance to slight differences in mutational effects on autophosphorylation versus casein phosphorylation.)

**Thermolability of F10 protein kinase activity in vitro.** Stabilities of the wild-type and mutant kinase activities were tested by preincubation of the purified enzyme preparations for 5 min at either 14, 25, 31, 37, or 42°C, followed by quenching on ice. The samples were then assayed for casein kinase activity at 25°C. The wild-type F10 kinase activity was stable to preincubation at 25°C, reduced by treatment at 31°C, and virtually abolished by preincubation at  $\geq 37^\circ\text{C}$  (Fig. 15A). (The purified wild-type F10 kinase was apparently unstable in vitro at temperatures normally permissive for vaccinia virus replication in vivo. This point is considered in Discussion.) The purified *ts61* F10 was somewhat more sensitive to incubation at 14 to 25°C but otherwise displayed a heat inactivation profile that was similar to that of the wild-type protein from 30 to 42°C (Fig. 15A). In contrast, the purified *ts54* kinase was clearly thermolabile; its inactivation curve was shifted to the left by about 10°C (Fig. 15A). Thus, the *ts54* kinase was almost completely inactivated by incubation at 31°C, whereas wild-type and *ts61* proteins retained 60% of the kinase activity of the untreated controls. The lability of the *ts54* protein at 25°C may account, in part, for the observed lower specific activity of the purified enzyme (e.g., because of destabilization of the enzyme during

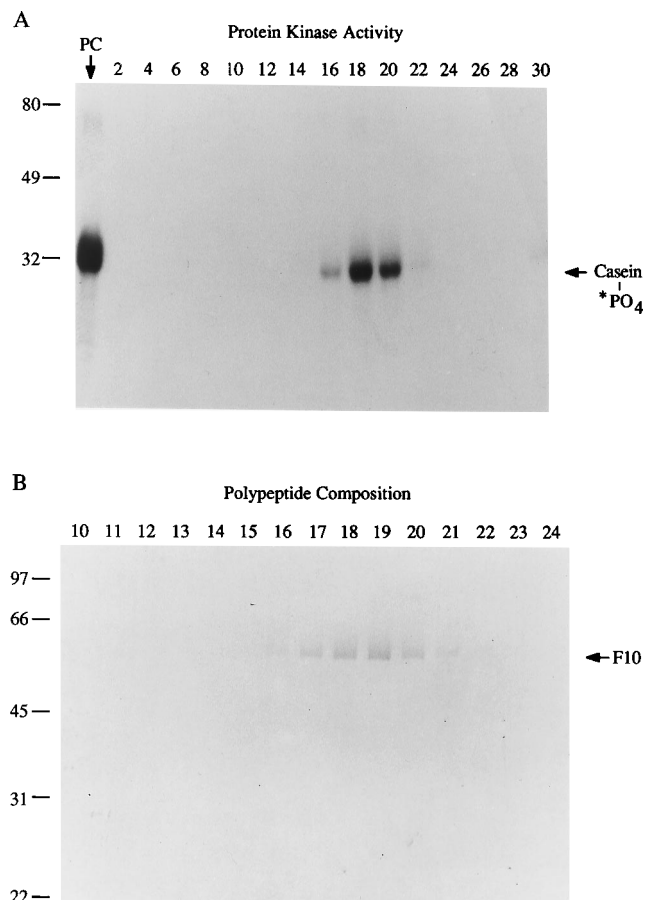


FIG. 11. Glycerol gradient sedimentation. The phosphocellulose (PC) fraction of recombinant wild-type His-F10 was sedimented in a glycerol gradient as described in Materials and Methods. Thirty fractions were collected from the bottom of the gradient. (A) Protein kinase activity. Kinase assay mixtures (20 µl) contained 50 mM Tris HCl (pH 7.5), 5 mM MgCl<sub>2</sub>, 1 mM DTT, 10 µg of casein, 50 µM [ $\gamma$ -<sup>32</sup>P]ATP, and 1 µl of either the phosphocellulose F10 fraction or the indicated glycerol gradient fraction. After incubation for 10 min at 25°C, the samples were denatured with SDS and analyzed by SDS-PAGE. An autoradiograph of the gel is shown. The positions and sizes (in kilodaltons) of marker proteins are indicated on the left. The predominant 32-kDa phosphoprotein product, corresponding to phosphorylated casein, is indicated on the right. (B) Aliquots (40 µl) of the indicated glycerol gradient fractions were analyzed by SDS-PAGE. Polypeptides were visualized by staining the gel with Coomassie blue. The 54-kDa polypeptide corresponding to His-F10 is indicated on the right. Sedimentation markers (catalase and cytochrome c) were centrifuged in a parallel gradient (not shown).

the kinase assay). The possibility that loss of kinase activity during the preincubation might be caused by degradation of the protein was excluded by the control experiment shown in Fig. 10. Here, the enzyme preparations were preincubated at 41°C (sufficient to inactivate the kinase) and analyzed by SDS-PAGE; there was no decrease in the abundance of the 54-kDa His-F10 polypeptide and no appearance of polypeptides of lower molecular weight (Fig. 10).

Thermostability was also assessed by following the inactivation of the enzyme preparations as a function of duration of preincubation at a single temperature, 31°C. The purified wild-type and *ts61* F10 proteins were inactivated with virtually identical kinetics (half-life, approximately 10 min). In contrast, *ts54* F10 was destabilized much more rapidly (Fig. 15B). These data indicate that the *ts54* mutation, which results in vaccinia ts virus replication in vivo, also renders the F10 kinase activity thermolabile in

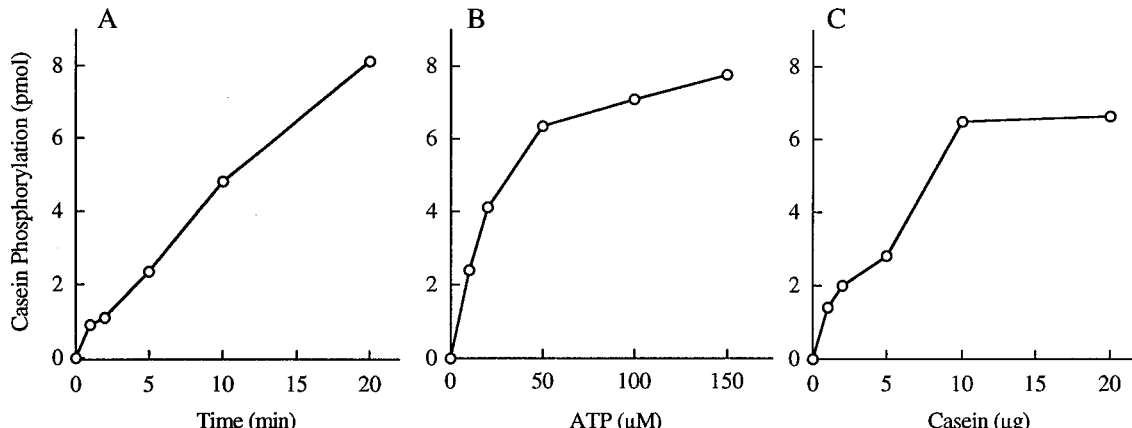


FIG. 12. Characterization of the F10 protein kinase activity. (A) Time course. A reaction mixture (120  $\mu$ l) containing 50 mM Tris HCl (pH 7.5), 5 mM MgCl<sub>2</sub>, 1 mM DTT, 60  $\mu$ g of casein, 50  $\mu$ M [ $\gamma$ -<sup>32</sup>P]ATP, and 84 ng of wild-type His-F10 was incubated at 25°C. Aliquots were withdrawn at the indicated times and quenched by addition of SDS. The reaction products were analyzed by SDS-PAGE. Casein phosphorylation was quantitated by scintillation counting. (B) ATP dependence. Reaction mixtures (20  $\mu$ l) containing 50 mM Tris HCl (pH 7.5), 5 mM MgCl<sub>2</sub>, 1 mM DTT, 10  $\mu$ g of casein, 14 ng of wild-type His-F10, and [ $\gamma$ -<sup>32</sup>P]ATP as indicated were incubated at 25°C for 10 min. Casein phosphorylation was quantitated by scintillation counting and plotted as a function of ATP concentration. (C) Casein dependence. Reaction mixtures (20  $\mu$ l) containing 50 mM Tris HCl (pH 7.5), 5 mM MgCl<sub>2</sub>, 1 mM DTT, 50  $\mu$ M [ $\gamma$ -<sup>32</sup>P]ATP, 14 ng of wild-type His-F10, and casein as indicated were incubated at 25°C for 10 min. Phosphorylation is plotted as a function of input casein.

vitro. In contrast, the stability of the purified *ts*61 F10 protein did not differ appreciably from that of the wild-type kinase in vitro.

## DISCUSSION

The mutations responsible for *ts* growth of vaccinia virus mutants *ts*28, *ts*54, *ts*61, and *ts*15 have been mapped by marker rescue to the F10 gene. The F10 gene product is a 52-kDa serine/threonine protein kinase that is encapsidated within the infectious virion (21). It has been named protein kinase 2, to distinguish this enzyme from the 34-kDa serine/threonine kinase encoded by the vaccinia virus B1 gene (22, 27). Although the B1 kinase is also present in the virus particle (22), the predominant protein kinase activity that can be isolated from virions is attributable to F10 (21, 22). Attempts to disrupt the F10 gene by insertion of a dominant selectable marker invari-

ably resulted in retention of a wild-type copy of the F10 gene in tandem with the disrupted allele (21). This implied that the F10 gene was essential for vaccinia virus replication but did not reveal the nature of its essential function. The present study of viral replication under nonpermissive growth conditions establishes that vaccinia virus protein kinase 2 is required at an early step of virus assembly.

Formation of the intracellular mature virion (IMV) in the cytoplasm of virus-infected cells is an event of extraordinary structural and biochemical complexity. It is no less elaborate than the assembly of a fully functional organelle. Structural intermediates are readily observed by electron microscopy, and they have been the subject of much interest and occasional controversy (7, 25, 29). The earliest viral structures are crescent-shaped membranes that progress to spherical forms encompassing viroplasm, a biochemically ill-defined substance

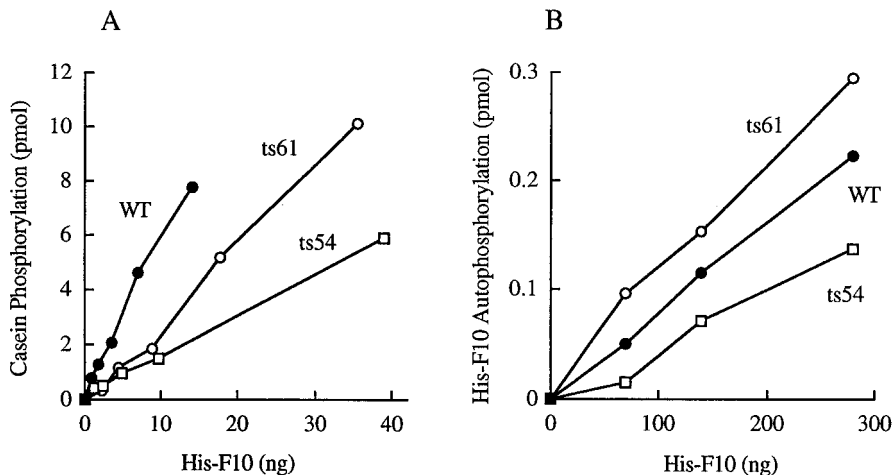


FIG. 13. Specific kinase activities of wild-type (WT) and mutant His-F10 proteins. (A) Casein kinase activity. Reaction mixtures (20  $\mu$ l) containing 50 mM Tris HCl (pH 7.5), 5 mM MgCl<sub>2</sub>, 1 mM DTT, 10  $\mu$ g of casein, 50  $\mu$ M [ $\gamma$ -<sup>32</sup>P]ATP, and purified recombinant His-F10 proteins as indicated (phosphocellulose fractions) were incubated for 10 min at 25°C. The reaction mixtures were analyzed by SDS-PAGE. Incorporation of <sup>32</sup>P into casein was quantitated by scintillation counting. (B) Autophosphorylation. Reaction mixtures (20  $\mu$ l) containing 50 mM Tris HCl (pH 7.5), 5 mM MgCl<sub>2</sub>, 1 mM DTT, 50  $\mu$ M [ $\gamma$ -<sup>32</sup>P]ATP, and His-F10 proteins as indicated (phosphocellulose fractions) were incubated for 10 min at 25°C. The reaction mixtures were analyzed by SDS-PAGE. Incorporation of <sup>32</sup>P into a 54-kDa species (presumed to be His-F10) was quantitated with a Phosphorimager.

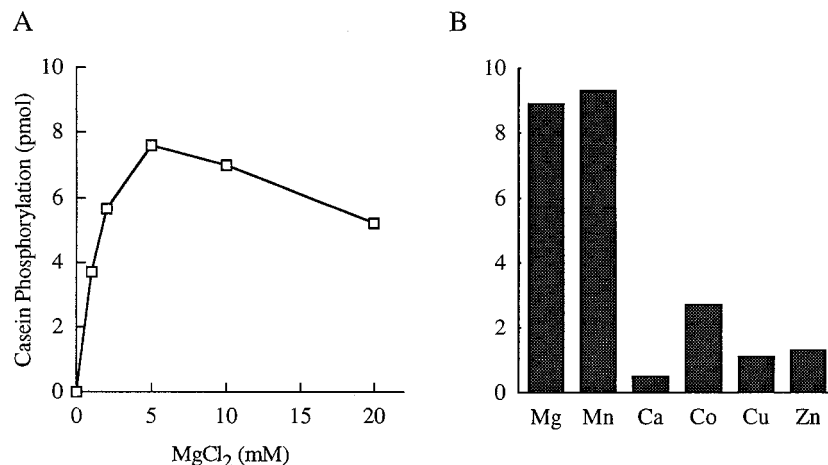


FIG. 14. Divalent-cation dependence. (A) Reaction mixtures (20  $\mu$ l) containing 50 mM Tris HCl (pH 7.5), 1 mM DTT, 10  $\mu$ g of casein, 50  $\mu$ M [ $\gamma$ -<sup>32</sup>P]ATP, 28 ng of wild-type His-F10, and MgCl<sub>2</sub> as indicated were incubated for 10 min at 25°C. (B) Reaction mixtures (20  $\mu$ l) contained 50 mM Tris HCl (pH 7.5), 1 mM DTT, 10  $\mu$ g of casein, 50  $\mu$ M [ $\gamma$ -<sup>32</sup>P]ATP, 28 ng of wild-type His-F10, and the divalent cations at 5 mM. Incubation was for 10 min at 25°C. Mg, Mn, Ca, and Co were added as chloride salts; Cu and Zn were added as sulfates.

that includes many of the structural proteins of the IMV. Although the immature particles appear circular in thin sections, they may not be fully enclosed. Microscopic evidence suggests that the viral genome is incorporated into the spherical immature particles through a pore-like opening (25). Closure of the spherical particles would occur after uptake of the DNA is complete. There then ensues a series of morphological transitions within the membrane-bound structures that lead ultimately to IMV. Known and presumptive events include condensation of the viral genome, proteolytic processing of major structural proteins, formation of the core and lateral bodies, and reorganization of the viral membranes. These steps are poorly understood, primarily because they have not been placed in the context of an ordered genetic or biochemical pathway.

*ts* mutations offer a potentially powerful genetic tool to study virus assembly. For example, Dales and coworkers have docu-

mented by electron microscopy altered patterns of morphogenesis when *ts* vaccinia virus mutants from their collection were grown under nonpermissive conditions (7). As many as 17 phenotypic categories were described on the basis of the types of viral structures accumulating at 40°C; these categories range in severity from mutants that formed no viral structures whatsoever (most severe) to those that formed progeny IMV particles that were morphologically normal but noninfectious (most subtle) (7). This collection remains a largely untapped resource, as most of the mutations have not, to our knowledge, been mapped to individual viral genes. The Condit *ts* collection has been mapped more thoroughly (6), but only a few of the mutants have provided direct insights into virus assembly. Mutations that affect viral macromolecular synthesis (either DNA replication or late gene expression) will invariably impact on virus assembly (e.g., see references 2, 15, and 37) because the

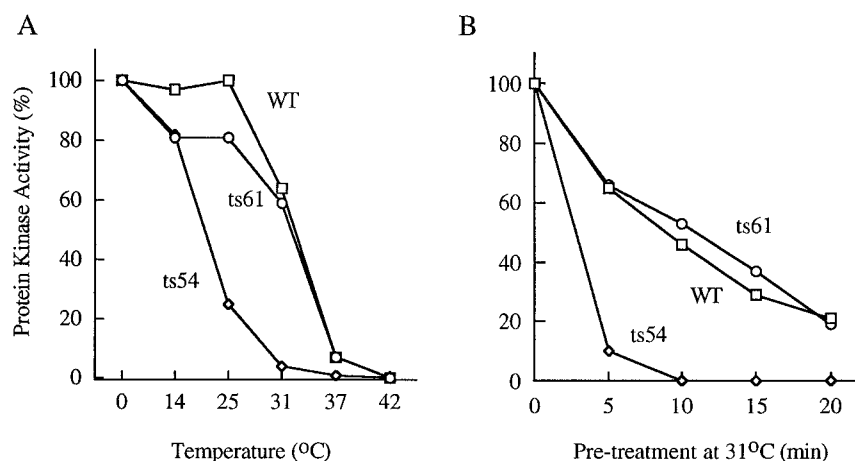


FIG. 15. Heat inactivation of protein kinase. (A) Samples of the purified wild-type (WT), ts61, and ts54 His-F10 preparations were preincubated in buffer A for 5 min at either 14, 25, 31, 37, or 42°C and then placed on ice. The residual casein kinase activity was assayed in reaction mixtures containing 50 mM Tris HCl (pH 7.5), 5 mM MgCl<sub>2</sub>, 1 mM DTT, 10  $\mu$ g of casein, 50  $\mu$ M [ $\gamma$ -<sup>32</sup>P]ATP, and 14 ng of preincubated His-F10 proteins. Casein kinase activity was normalized to that of control reactions containing a wild-type, ts61, or ts54 His-F10 that had not been subjected to preincubation. Activity (percent of control) is plotted against the temperature of preincubation (note the nonlinear scale on the x axis). (B) Samples of the purified wild-type, ts61, and ts54 His-F10 preparations were preincubated in buffer A at 31°C for the indicated times and then placed on ice. The residual casein kinase activity was assayed in reaction mixtures containing 50 mM Tris HCl (pH 7.5), 5 mM MgCl<sub>2</sub>, 1 mM DTT, 10  $\mu$ g of casein, 50  $\mu$ M [ $\gamma$ -<sup>32</sup>P]ATP, and 14 ng of preincubated His-F10 proteins as indicated. Casein kinase activity was normalized to that of control reactions containing a wild-type, ts61, or ts54 His-F10 that had not been subjected to preincubation. Activity (percent of control) is plotted as a function of the duration of preincubation.

initial formation of viral membranes depends on late protein synthesis (which is, in turn, contingent on DNA replication). Although formation of viroplasmic inclusions is not contingent on late gene expression, the microscopic appearance of the viroplasm formed by *ts* mutants can vary depending on the mutant strain.

The microscopic phenotype of the *ts* mutations in F10 is reminiscent of the category C of morphological aberrations described by Dales et al. (7). Because the three F10 *ts* mutants analyzed by electron microscopy showed a relatively consistent morphogenetic defect and because all of the F10 *ts* mutants synthesized late proteins at the nonpermissive temperature, we infer that the phenotype was a direct consequence of the production of defective F10 protein. Indeed, each *ts* virus had sustained a distinctive nucleotide change resulting in different single-amino-acid substitutions in the F10 protein.

The F10 *ts* mutations demarcate the earliest genetically defined step in vaccinia virus assembly. The F10 gene product apparently acts prior to the D13 protein, which is the target of the drug rifampin (1, 23). The D13-dependent step was, until now, the most proximal assembly event that had been studied genetically and pharmacologically. Rifampin causes assembly to undergo arrest after the formation of abnormal membrane-enclosed structures (rifampin bodies), which contain viroplasm but lack the rigid spherical shape of normal immature particles. The rifampin bodies appear to lack the spicule layer characteristic of the normal immature forms. Rifampin resistance and hypersensitivity are attributable to point mutations in the D13 gene (1, 23), which encodes a 65-kDa polypeptide. The D13 protein localizes by immunoelectron microscopy to the concave surface of the membrane crescents and the internal face of the immature spherical particles (30, 34). In the presence of rifampin, the D13 protein is found in viroplasmic inclusions but not in association with membranes (24, 30). The rifampin bodies rapidly acquire a rigid spicule-containing spherical structure upon removal of the drug. Conditional repression of D13 gene expression elicits a morphogenetic phenotype similar to that elicited by rifampin treatment (39). It has been suggested that the D13 polypeptide serves as a scaffold to impart curvature to the membrane crescents (30). The proposition that F10 acts prior to D13 is based on the following: (i) the F10 phenotype results only in scant formation of membrane crescents, whereas the D13 phenotype permits abundant production of membranous structures, albeit malformed ones; (ii) membrane closure is rare in the F10 mutants but does occur when D13 function is blocked; (iii) the few membranes formed by the F10 mutants do not encapsidate viroplasm, whereas viroplasm is incorporated into rifampin bodies. Conceivably, the order of action of F10 and D13 could be tested directly with the F10 *ts* mutants, e.g., by combining temperature shifts with rifampin block and reversal. Such approaches may be complicated, however, by a requirement for F10 action at additional downstream steps in virus assembly.

How might the F10 protein participate in early viral assembly? The membrane crescents are believed to derive from the intermediate compartment, a membrane cisterna situated in the vesicular trafficking pathway between the endoplasmic reticulum and the Golgi stacks (29). The proteins that dictate the highly ordered and rigid shape of the viral membranes remain largely undefined (except for D13, as noted above). The intermediate-compartment hypothesis must invoke some molecular "cement" that bridges the two membranes and obliterates the lumen. This could be accomplished either by a single viral protein that transits through both membranes or by two separate proteins that make contact across the lumen. There must be some asymmetry of the fused membrane structure that

facilitates the acquisition of curvature, e.g., a specific ligand on the concave face of the crescents which interacts (perhaps) with the D13 protein or some other partner. The F10 mutations markedly reduce the extent of crescent formation as well as progression to spherical forms. The most appealing hypothesis is that the protein kinase activity of the F10 protein is affected at the nonpermissive temperature and that the observed assembly defect results from a failure to phosphorylate one or more viral proteins involved in membrane formation. Any number of specific models can be invoked, e.g., that phosphorylation is required to target viral proteins to the intermediate compartment, to promote closure of the membrane cisterna, or to recruit scaffold proteins to one or another face of the intermediate compartment. Because the vaccinia virus proteins targeted to the intermediate compartment have not yet been identified, it is difficult to test these ideas directly.

The notion that the protein kinase activity of F10 is relevant to its biological function is supported by our studies showing that the *ts*54 F10 protein kinase is thermolabile in vitro. However, the *ts* phenotype *in vivo* may result from any of several distinct mechanisms not predicated on *ts* catalytic activity, for example, (i) enhanced turnover of the mutant F10 polypeptide at the nonpermissive temperature or (ii) defective interaction of F10 kinase with other viral proteins, including potential regulatory factors or specific phosphate acceptors. Interaction of the F10 protein with other polypeptides may serve to stabilize the kinase *in vivo* and would explain the observation that even the wild-type F10 was relatively unstable in vitro at physiological temperatures. No matter what basis is established for functional inactivation at the nonpermissive temperature, the major issue will be the identification of the target proteins that are phosphorylated by protein kinase 2 *in vivo*. One obvious approach will be to follow the incorporation of labeled phosphate into protein by cells infected with the various F10-*ts* viruses at permissive and nonpermissive temperatures. However, given the background of multiple cellular protein kinases and the existence of at least one other vaccinia virus-encoded protein kinase, the *in vivo* phosphorylation pattern may be difficult to interpret.

Several vaccinia virus-encoded proteins are phosphorylated *in vivo*. Prominent among these is an 11-kDa phosphoprotein (encoded by the F17 gene [16]) that is encapsidated within the infectious IMV. The 11-kDa protein, which binds to DNA, is a major structural component of the virion and is phosphorylated *in vivo* at two different serine residues (19). An 11-kDa polypeptide (presumably F17) is among the most prominent of the virion polypeptides that are phosphorylated *in vitro* by the intrinsic protein kinase activity of the vaccinia virus core. The fact that vaccinia virus also encodes a phosphoprotein phosphatase (14) makes it likely that protein phosphorylation is a dynamic process *in vivo*. A long-standing hypothesis is that phosphorylation of virion proteins (including the 11-kDa species) by the endogenous kinase might be required to activate the transcription of early viral genes by the virion-associated vaccinia virus RNA polymerase. Our findings concerning the F10 *ts* mutants do not exclude such a role for protein kinase 2, but they do make clear that faulty transcription by progeny virions is not the basis for the *ts* phenotype. Although the 11-kDa protein remains a plausible substrate for vaccinia virus protein kinase 2, it is again unlikely that failure to phosphorylate F17 would account for the phenotypes observed for F10 *ts* mutants at the nonpermissive temperature. It is known, for example, that a conditional null mutant of the gene encoding the 11-kDa phosphoprotein results in a morphogenetic block subsequent to formation of the spherical immature particles

(38), i.e., at a stage downstream of the F10 *ts* arrest observed in the present work.

The crescent assembly step is apparently the earliest event that requires F10; whether other morphogenetic steps also entail F10 action (e.g., via phosphorylation of different virion components at distinct stages of assembly) is an issue that is not addressed herein but may be approached by performing temperature shifts at different times after infection or by seeking more subtle phenotypes at semipermissive temperatures. Some pleiotropy of the F10 phenotype was revealed by the present study, e.g., the allele-specific effects on proteolytic processing of the major virion structural proteins 4a and 4b. Numerous prior studies have shown that almost any drug treatment or genetic mutation that affects morphogenesis at the microscopic level is associated with some defect in protein processing. This is because processing of p4a and p4b is likely to occur at a late stage of internal maturation of the virion and therefore be affected by numerous upstream defects. The observation that *ts*61 processed p4b to some extent at the non-permissive temperature despite the profound early assembly defect suggests that morphogenetic steps do not proceed in a strictly linear path. Rather, parallel pathways (e.g., membrane formation, genome condensation, and protein processing) may converge during virion assembly without being strictly coupled.

In conclusion, this study provides the first suggestion that a protein kinase (and, by inference, protein phosphorylation) is essential for vaccinia virus morphogenesis. Our results underscore the value of the existing collection of *ts* vaccinia virus mutants in defining a multistep, multicomponent assembly pathway.

#### REFERENCES

- Baldick, C. J., and B. Moss. 1987. Resistance of vaccinia virus to rifampin conferred by a single nucleotide substitution near the predicted amino terminus of a gene encoding an Mr 62,000 polypeptide. *Virology* **156**:138–145.
- Carpenter, M. S., and A. M. DeLange. 1992. Identification of a temperature-sensitive mutant of vaccinia virus defective in late but not intermediate gene expression. *Virology* **188**:233–244.
- Christen, L., M. A. Higman, and E. G. Niles. 1992. Phenotypic characterization of three temperature-sensitive mutations in the vaccinia virus early gene transcription factor. *J. Gen. Virol.* **73**:3155–3167.
- Condit, R. C., and A. Motyczka. 1981. Isolation and preliminary characterization of temperature-sensitive mutants of vaccinia virus. *Virology* **113**:224–241.
- Condit, R. C., A. Motyczka, and G. Spizz. 1983. Isolation, characterization, and physical mapping of temperature-sensitive mutants of vaccinia virus. *Virology* **128**:429–443.
- Condit, R. C., and E. G. Niles. 1990. Orthopoxvirus genetics. *Curr. Top. Microbiol. Immunol.* **163**:1–35.
- Dales, S., V. Milanovitch, B. G. T. Pogo, S. B. Weintraub, T. Huima, S. Wilton, and G. McFadden. 1978. Biogenesis of vaccinia: isolation of conditional lethal mutants and electron microscopic characterization of their phenotypically expressed defects. *Virology* **84**:403–428.
- Davison, A. J., and B. Moss. 1989. Structure of vaccinia virus late promoters. *J. Mol. Biol.* **210**:771–784.
- Drillien, R., D. Spehner, and A. Kirn. 1982. Complementation and genetic linkage between vaccinia virus temperature-sensitive mutants. *Virology* **119**:372–381.
- Dyster, L. M., and E. G. Niles. 1991. Genetic and biochemical characterization of vaccinia virus genes D2L and D3R which encode virion structural proteins. *Virology* **182**:455–467.
- Ensinger, M. J. 1982. Isolation and genetic characterization of temperature-sensitive mutants of vaccinia virus WR. *J. Virol.* **43**:778–790.
- Fathi, Z., and R. C. Condit. 1991. Phenotypic characterization of a vaccinia virus temperature-sensitive complementation group affecting a virion component. *Virology* **181**:273–276.
- Goebel, S. J., G. P. Johnson, M. E. Perkus, S. W. Davis, J. P. Winslow, and E. Paoletti. 1990. The complete sequence of vaccinia virus. *Virology* **179**:247–266.
- Guan, K., S. S. Broyles, and J. E. Dixon. 1991. A Tyr/Ser protein phosphatase encoded by vaccinia virus. *Nature (London)* **350**:359–362.
- Hooda-Dhingra, U., C. L. Thompson, and R. C. Condit. 1989. Detailed phenotypic characterization of five temperature-sensitive mutants in the 22- and 147-kDa subunits of vaccinia virus DNA-dependent RNA polymerase. *J. Virol.* **63**:714–729.
- Johnson, G. P., S. J. Goebel, and E. Paoletti. 1993. An update on the vaccinia virus genome. *Virology* **196**:381–401.
- Kane, E. M., and S. Shuman. 1992. Temperature-sensitive mutations in the vaccinia virus H4 gene encoding a component of the virion RNA polymerase. *J. Virol.* **66**:5752–5762.
- Kane, E. M., and S. Shuman. 1993. Vaccinia virus morphogenesis is blocked by a temperature-sensitive mutation in the I7 gene that encodes a virion component. *J. Virol.* **67**:2689–2698.
- Kao, S., and W. R. Bauer. 1987. Biosynthesis and phosphorylation of vaccinia virus structural protein VP11. *Virology* **159**:399–407.
- Li, J., M. J. Pennington, and S. S. Broyles. 1994. Temperature-sensitive mutations in the gene encoding the small subunit of the vaccinia virus early transcription factor impair promoter binding, transcription activation, and packaging of multiple virion components. *J. Virol.* **68**:2605–2614.
- Lin, S., and S. S. Broyles. 1994. Vaccinia protein kinase 2: a second essential serine/threonine protein kinase encoded by vaccinia virus. *Proc. Natl. Acad. Sci. USA* **91**:7653–7657.
- Lin, S., W. Chen, and S. S. Broyles. 1992. The vaccinia virus B1R gene product is a serine/threonine protein kinase. *J. Virol.* **66**:2717–2723.
- McNulty-Kowalczyk, A., and E. Paoletti. 1993. Mutations in ORF D13 and other genetic loci alter the rifampin phenotype of vaccinia virus. *Virology* **194**:638–646.
- Miner, J. N., and D. E. Hruby. 1989. Rifampin prevents virosome localization of L65, an essential vaccinia virus polypeptide. *Virology* **170**:227–237.
- Morgan, C. 1976. Vaccinia virus reexamined: development and release. *Virology* **73**:43–58.
- Paoletti, E., and B. Moss. 1972. Protein kinase and specific phosphate acceptor proteins associated with vaccinia virus cores. *J. Virol.* **10**:417–424.
- Rempel, R. E., and P. Traktman. 1992. Vaccinia virus B1 kinase: phenotypic analysis of temperature-sensitive mutants and enzymatic characterization of recombinant proteins. *J. Virol.* **66**:4413–4426.
- Shuman, S. 1992. Vaccinia virus RNA helicase: an essential enzyme related to the DE-H family of RNA-dependent NTPases. *Proc. Natl. Acad. Sci. USA* **89**:10935–10939.
- Sodeik, B., R. W. Doms, M. Ericsson, G. Hiller, C. E. Machamer, W. van't Hof, G. van Meer, B. Moss, and G. Griffiths. 1993. Assembly of vaccinia virus: role of the intermediate compartment between the endoplasmic reticulum and the Golgi stacks. *J. Cell Biol.* **121**:521–541.
- Sodeik, B., G. Griffiths, M. Ericsson, B. Moss, and R. W. Doms. 1994. Assembly of vaccinia virus: effects of rifampin on the intracellular distribution of viral protein p65. *J. Virol.* **68**:1103–1114.
- Takahashi, T., M. Oie, and Y. Ichihashi. 1994. N-terminal amino acid sequences of vaccinia virus structural proteins. *Virology* **202**:844–852.
- Thompson, C. L., and R. C. Condit. 1986. Marker rescue mapping of vaccinia virus temperature-sensitive mutants using overlapping cosmid clones representing the entire virus genome. *Virology* **150**:10–20.
- VanSlyke, J. K., C. A. Franke, and D. E. Hruby. 1991. Proteolytic maturation of vaccinia virus core proteins: identification of a conserved motif at the N termini of the 4b and 25K virion proteins. *J. Gen. Virol.* **72**:411–416.
- VanSlyke, J. K., and D. E. Hruby. 1994. Immunolocalization of vaccinia virus structural proteins during virion formation. *Virology* **198**:624–635.
- VanSlyke, J. K., S. S. Whitehead, E. M. Wilson, and D. E. Hruby. 1991. The multistep proteolytic maturation pathway utilized by vaccinia virus P4a protein: a degenerate conserved cleavage motif within core proteins. *Virology* **183**:467–478.
- Zhang, Y., B. Ahn, and B. Moss. 1994. Targeting of a multicomponent transcription apparatus into assembling vaccinia virus particles requires RAP94, an RNA polymerase-associated protein. *J. Virol.* **68**:1360–1370.
- Zhang, Y., J. G. Keck, and B. Moss. 1992. Transcription of viral late genes is dependent on expression of the viral intermediate gene G8R in cells infected with an inducible conditional-lethal mutant vaccinia virus. *J. Virol.* **66**:6470–6479.
- Zhang, Y., and B. Moss. 1991. Vaccinia virus morphogenesis is interrupted when expression of the gene encoding an 11-kilodalton phosphorylated protein is prevented by the *Escherichia coli lac* repressor. *J. Virol.* **65**:6101–6110.
- Zhang, Y., and B. Moss. 1992. Immature viral particle formation is interrupted at the same stage by lac operator-mediated repression of the vaccinia virus D13L gene and by the drug rifampin. *Virology* **187**:643–653.